TITLE PAGE

Citation Format:

J. Zouaoui, L. Hervé, L. Di Sieno, A. Planat-Chrétien, M. Berger, A. Dalla Mora, A. Pifferi, J. Derouard, J.-M. Dinten, "In-depth quantification by using multispectral time-resolved diffuse optical tomography," Diffuse Optical Imaging V, edited by H. Dehghani, P. Taroni, Proc. of SPIE Vol. 9538, 95380C, 2015

Copyright notice:

DOI abstract link:

http://dx.doi.org/10.1117/12.2183819

In-depth quantification by using Multispectral Time-Resolved Diffuse Optical Tomography

Judy Zouaoui[a*], Lionel Hervé[a], Laura Di Sieno[c], Anne Planat-Chrétien[a], Michel Berger[a], Alberto Dalla Mora[c], Antonio Pifferi[c], Jacques Derouard[b] and Jean-Marc Dinten[a]
[a]Univ. Grenoble Alpes, F-38000 Grenoble, France
CEA, LETI, MINATEC Campus, F-38054 Grenoble, France
[b]Univ. Grenoble Alpes, LIPhy, F-38000 Grenoble, France
[c]Politecnico di Milano, Dipartimento di Fisica, Piazza Leonardo da Vinci 32, Milano I-20133, Italy

ABSTRACT

Near-infrared diffuse optical tomography (DOT) is a medical imaging which gives the distribution of the optical properties of biological tissues. To obtain endogenous chromophore features in the depth of a scattering medium, a multiwavelength/time-resolved (MW/TR) DOT setup was used. Reconstructions of the three-dimensional maps of chromophore concentrations of probed media were obtained by using a data processing technique which manages Mellin-Laplace Transforms of their MW/TR optical signals and those of a known reference medium. The point was to put a constraint on the medium absorption coefficient by using a material basis composed of a given set of chromophores of known absorption spectra. Experimental measurements were conducted by injecting the light of a picosecond near-infrared laser in the medium of interest and by collecting, for several wavelengths and multiple positions, the backscattered light via two fibers (with a source-detector separation of 15 mm) connected to fast-gated single-photon avalanche diodes (SPAD) and coupled to a time-correlated single-photon counting (TCSPC) system. Validations of the method were performed in simulation in the same configuration as the experiments for different combination of chromophores. Evaluation of the technique in real conditions was investigated on liquid phantoms composed of an homogenous background and a 10 mm depth inclusion formed of combination of intralipid and inks scanned at 30 positions and at three wavelengths. Both numerical and preliminary phantom experiments confirm the potential of this method to determine chromophore concentrations in the depth of biological tissues.

Keywords: diffuse optical tomography, time-resolved, multispectral, quantification, Mellin-Laplace transform

INTRODUCTION

Diffuse optical tomography (DOT) [1] is a medical imaging technique that consists in reconstructing the three-dimensional (3D) maps of the distribution of optical properties of biological tissues inside an organ with external optical measurements. To analyze highly diffusive biological tissues, such as living brains or breasts [2], reflectance measurements are obtained with near-infrared light. To separate endogenous chromophores as oxy and deoxy-hemoglobin (HbO_2 and Hb) which have distinct spectra signatures, multiwavelength (MW) acquisitions are required. In reflectance geometry, time-resolved (TR) measurements are appropriate to collect late photons so that information in depth can be recovered [3].

We developed a new method that enables to quantify and determine the spatial distribution of endogeneous chromophores in depth from MW/TR optical setup associated with a 3D reconstruction algorithm. The point was to put a constraint on the medium absorption coefficient by using a material basis composed of a given set of chromophores of known absorption spectra.

In this study, simulations were conducted with different chromophore combinations and two different depths. They permitted to validate our method. In addition, phantom experiments were carried out to evaluate the method in real conditions. Preliminary results show the potential of this technique.

*judy.zouaoui@cea.fr; phone 0033438780363; www.cea-tech.fr

Diffuse Optical Imaging V, edited by Hamid Dehghani, Paola Taroni, Proc. of SPIE Vol. 9538, 95380C · © 2015 SPIE · CCC code: 1605-7422/15/$18 · doi: 10.1117/12.2183819

METHOD

To obtain the chromophore decomposition of an unknown medium *B* on a material basis with DOT technique, we acquire two sets, $M_{sd}^{A\lambda}(t)$ and $M_{sd}^{B\lambda}(t)$, of multi-wavelength (indexed by λ) time-domain measurements on a known reference medium A and on the unknown chromophore composition medium *B* for a collection of source (indexed by *s*) and detector (indexed by *d*) positions.

The media A and B are discretized on a mesh grid with nodes (indexed by *m*) at position $\vec{r}_m$. By assuming the diffusion approximation, and using the Mellin-Laplace Transform (MLT) [4] (indexed by *n*) of TR measurements, and the expression of the total absorption coefficient ($\mu_m^\lambda = \sum_i S_i^\lambda C_m^i$, where μ_m^λ is the total absorption coefficient, S_i^λ is the matrix containing reference molecular extinction coefficients of a material basis, C_m^i are the chromophore concentrations, and *i* is the chromophore index) and the combination of measurements [3] $\delta M_{sd}^{\lambda n(k)}$, we end up with the formula which links (for small variations) measurements with the chomophore concentration update:

$$\delta M_{sd}^{\lambda n(k)} = \sum_{m,i} W_{sdi}^{\lambda nm(k)} \delta C_m^{i(k)} \tag{1}$$

where the update $\delta C_m^{i(k)}$ is the difference between the true chromophore concentration C_m^i of medium *B* and the chromophore concentration $C_m^{i(k)}$ obtained at iteration *k*. The combination of measurements $\delta M_{sd}^{\lambda n}$ is:

$$\delta M_{sd}^{\lambda n(k)} = M_{sd}^{B\lambda n} * G_{sd}^{A\lambda n} - M_{sd}^{A\lambda n} * G_{sd}^{B\lambda n(k)} \tag{2}$$

where '*' is the convolution product (on *n*) and $G_{sd}^{A\lambda n}$ and $G_{sd}^{B\lambda n(k)}$ are the MLT of Green's function of the diffusion equation evaluated between source *s* and detector *d* with the concentration $C_m^{i(k)}$ obtained at iteration *k*. The sensitivity matrix $W_{sdi}^{\lambda nm(k)}$ is:

$$W_{sdi}^{\lambda nm(k)} = -M_{sd}^{A\lambda n} * G_{sm}^{B\lambda n(k)} * G_{dm}^{B\lambda n(k)} S_i^\lambda V_m \tag{3}$$

where V_m is the volume affected node *m* and $G_{sm}^{B\lambda n(k)}$ and $G_{dm}^{B\lambda n(k)}$ are the Green's function of medium *B* for source *s* or detector *d* evaluated at position r_m.

The matrix S_i^λ allows us to constrain the problem to a valid combination of chromophore concentrations in medium B. For example, it can be built with reference molecular extinction coefficients of HbO_2 and Hb**.**

By solving Eq. (1), we get an update of the chromophore concentrations ($C_m^{i(k+1)} = C_m^{i(k)} + \delta C_m^{i(k)}$). The process is repeated until convergence.

EXPERIMENTAL SETUP

The method has been assessed on liquid diffusive phantom experiments. The background medium was made up of a mixture of water, intralipid (Frenesius Kabi) and black ink (China ink, Rotring). The inclusion was a hollow resin 8 mm diameter cylinder filled with water, intralipid and blue ink (Colori mordenti per legno, gouro blue). This inclusion was immersed at 10 mm depth. The scattering coefficient was the same for the background medium and the inclusion (μ_s' =12 cm^{-1} at 750 nm).

The experimental measurements were conducted by injecting single wavelength light pulses emitted by a supercontinuum laser (SuperK Extreme, NKT Photonics, 70 ps pulse width, 40 MHz repetition rate) in the phantom through an optical fiber. Thanks to an Acousto-Optical Tunable Filter (AOTF, NKT Photonics), the wavelength was selected in the range from 690 nm to 850 nm and could be fast switched. The backscattered light was collected by two optical fibers at a distance of 15 mm from the excitation fiber (see Fig. 1). Each collection fibers were connected to two different fast-gated SPADs [5, 6, 7] coupled to a TCSPC system.

The phantom scan was performed by moving the block of the three fibers on 6 × 5 positions (distance between two points: 0.75 cm for both directions, see Fig. 1). Then the scan was repeated for each wavelength and on each liquid phantom without and with the inclusion.

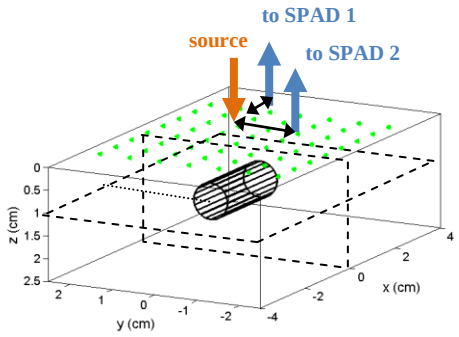

Figure 1. Drawing of the phantom and scan set-up composed of one source (orange) and two detectors fibers (blue) whose relative distances are fixed while they are positioned successively on the green spots.

RESULTS

Numerical considerations

Here we computed the Green's function by using the finite volume method on the discretized medium (10478 nodes, 6×5×2.5 cm^3 medium dimensions) as in [8]. The solving of Eq. (1) was obtained by using the conjugated gradient (5 iterations). The photon noise on the measurements was taken into consideration to weight the data. Ten general iterations with chromophore concentration updates were performed.

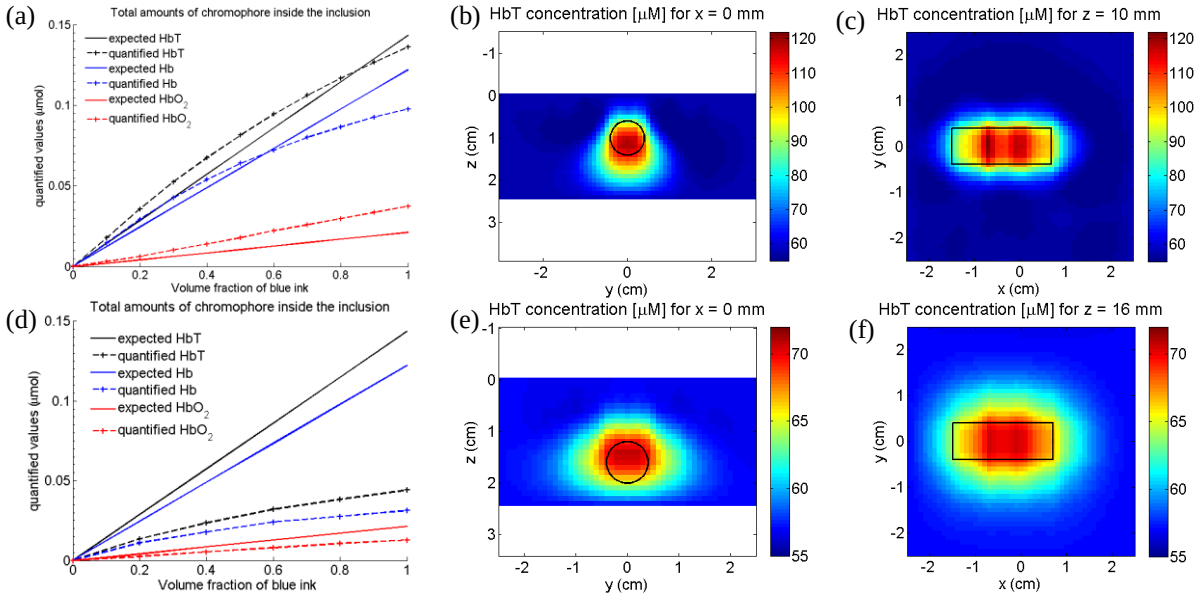

Figure 2. Quantification of the reconstructed amount of HbT, Hb and HbO_2 of the inclusion at (a) 10 mm and (d) 16 mm depth in simulation. Reconstructed concentration distribution of HbT for (b) x = 0 mm and for (c) z = 10 mm deduced from the numerical simulation of the true experiment with the inclusion at 10 mm. Simulated reconstructed concentration distribution of HbT for (e) x = 0 mm and for (f) z = 16 mm with the inclusion at 16 mm depth. Continuous black line is the true inclusion position.

From the reconstruction, all quantities were expressed as Hb/HbO_2 equivalents or HbT by summing Hb and HbO_2 quantities. To estimate the quantification, we calculated the total amount of substances inside the inclusion, expressed as the integral of its reconstructed concentration where the integration support was defined as the volume with all concentration values above 30% of the difference between the maximum reconstructed concentration value and the background reconstructed concentration value.

Simulations

In order to compare with the experimental results and to explore more chromophore compositions, we carried out simulations in the same configuration as the experiments and by including the experimental instrumental response function (IRF) of the SPAD enabled in fast-gated mode. In these simulations, different combinations of blue and black ink in the inclusion by varying the volume fraction of blue ink from 0 to 1 and inversely for black ink (1 to 0) were tested. Two depth were simulated 10 and 16 mm. Simulations were realized with three wavelengths (750, 800 and 850 nm).

Figure 2 (a) and (d) shows the behaviors of the quantified amounts of HbT, Hb and HbO_2 inside the inclusion at 10 mm and 16 mm depth compared with the expected values for the different material combinations. Good quantification of HbT, Hb and HbO_2 is obtained for 10 mm. We have a significant decrease of the quantification of the three components with the inclusion of 16 mm depth but we can still distinguish them. For the same material composition as experiment (i.e. a volume fraction of blue ink of 1 μ_a(750 nm)= 0.5 cm^{-1}), the quantified amount of HbT is 0.136 µmol for 10 mm depth which is in agreement with the expected one, 0.143 µmol. In Figs 2(b), (c), (e) and (f), two slices (slice z-y and slice y-x) for 10 mm and 16 mm inclusion depth show the three-dimensional chromophore decomposition of HbT for the same material combination than experiment. For the simulation, the reconstruction is focused on the wanted place and chromophore quantifications are correct for the whole studied range for 10 mm. When the inclusion is deeper at 16 mm, the reconstruction is also focused on the wanted place but more spread and the maximum reconstructed concentration is 40% less than for the inclusion at 10 mm depth.

Experiments

Here, we present results carried out on a phantom consisting of a black-ink background (μ_a(750 nm) = 0.1 cm^{-1} which corresponds to $25S_{Hb}^{\lambda} + 32S_{HbO_2}^{\lambda}$) and a blue-ink 2.2 cm-length inclusion (μ_a(750 nm)= 0.5 cm^{-1} which corresponds to $136S_{Hb}^{\lambda} + 51S_{HbO_2}^{\lambda}$) at 10 mm depth (Fig. 1). The phantom was scanned at three different wavelengths (750, 800 and 850 nm). For the fast-gated SPAD acquisition, we acquire photons using gates opening at different delays in order to record only selected portion of the time-resolved curves. The first gate was chosen so that it is opened before the first re-emitted photon is collected and closed after the last photons are recorded. In this mode the full distribution of re-emitted photons temporally fits in the gate making this measurement comparable to that performed with a free-running detector. For this reason, we can operate performance comparison between the gated mode vs. the non-gated mode for the quantification of an absorbing inclusion.

Figure 3 illustrates this comparison with three-dimensional representations of HbT distribution and the distribution of the oxygen saturation (SO_2) in percent which is the ratio of HbO_2 and HbT. For both modes, we have a good localization of the inclusion. We observe fewer spreading problems around the inclusion and a more focus position of the inclusion in the gated mode. Concerning the quantification, the expected values are 57 µM of HbT and 56 % of SO_2 for the background and 187 µM of HbT and 27 % of SO_2 for the inclusion. For both modes, we obtain a good quantification and a good depth reconstruction. In paper [5], it was already been revealed that for an inclusion at 10 mm depth the non-gated and gated acquisitions give the same depth reconstruction but here we can see that of this depth we are a small improvement in quantification and focus of the reconstruction with gating mode. Compared to simulation (Fig 2 (b) and (c)), reconstructions with the gated mode (Fig 3 (b)) have the same amplitude in HbT concentration but in the experiment we see spreading problems in the z-axis which may be caused by erroneous reconstruction values in depth where late photons are involved. Such spreading led to overestimation of all chromophore quantities (quantified amount of HbT is 0.4 µmol instead of 0.14 µmol as expected).

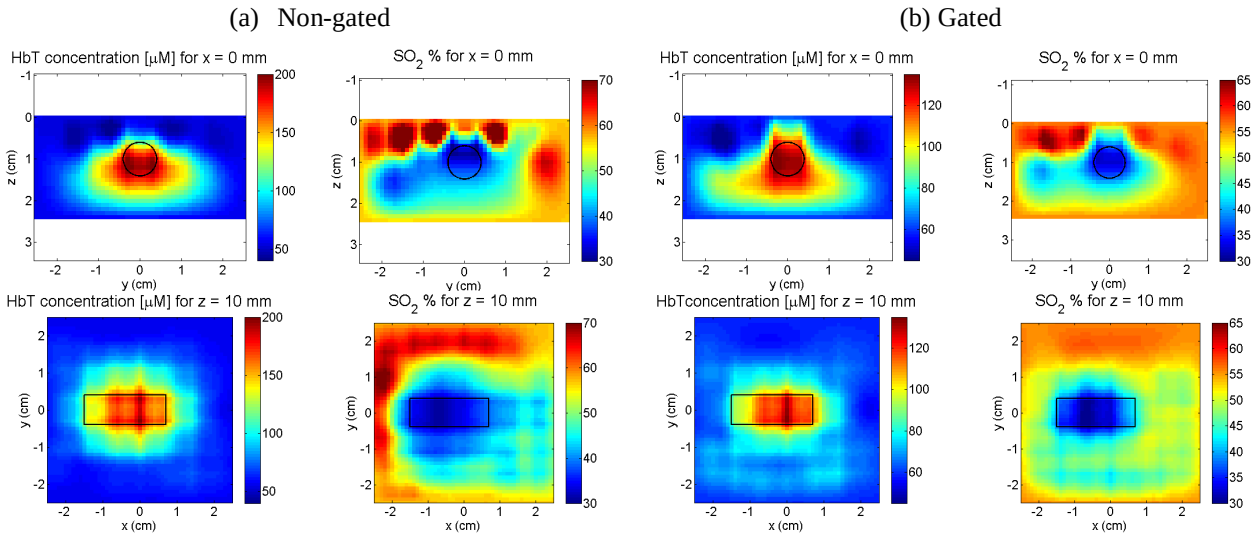

Figure 3. Comparison between (a) non-gated and (b) gated modes on reconstructed concentration maps of HbT and SO_2. First line corresponds to slice z-y with x = 0 mm. Second line corresponds to slice y-x with z = 10 mm.

CONCLUSION

To resolve the problem of quantification in depth in DOT, we proposed an MW/TR instrumentation combined to a reconstruction method base on the use of MLT and material basis.

Simulations have permitted to validate our method for different combination of chromophores. Correct localization and good quantification for 10 mm depth have been obtained. A dedicated experiment with an adapted instrumentation that enables to exploit long time of flight photons has showed the potential of the technique.

However, spreading problems have been identified which disturb the quantification and localization of the heterogeneities in a medium. In simulation, the effect of depth on the quantification was highlighted and shows that there is a real challenge for DOT to quantify in depth.

A complete experimental study is currently investigated to estimate the effect of the depth on quantification and will be taking into account in the reconstruction method.

ACKNOWLEDGEMENTS

This work was performed within the framework of the LABEX PRIMES (ANR-11-LABX-0063) of Université de Lyon, within the program "Investissements d'Avenir" (ANR-11-IDEX-0007) operated by the French National Research Agency (ANR).

REFERENCES

[1] Durduran, T., Choe, R., Baker, W. B., & Yodh, A. G., "Diffuse optics for tissue monitoring and tomography, " Reports on Progress in Physics, *73*(7), 076701 (2010).

[2] Quarto, G., Spinelli, L.; Pifferi, A., Torricelli, A., Cubeddu, R., Abbate, F., Balestreri, N., Menna, S., Cassano, E., and Taroni, P., "Estimate of tissue composition in malignant and benign breast lesions by time-domain optical mammography," Biomed. Opt. Express 5, 3684-3698 (2014).

[3] Puszka, A., Hervé, L., Planat-Chrétien, A., Koenig, A., Derouard, J., and Dinten, J.-M., "Time-domain reflectance diffuse optical tomography with Mellin-Laplace transform for experimental detection and depth localization of a single absorbing inclusion," Biomed. Opt. Express 4, 569-583 (2013).
[4] Hervé, L., Puszka, A., Planat-Chrétien, A., and Dinten, J.-M., "Time-domain diffuse optical tomography processing by using the Mellin–Laplace transform," Appl. Opt., 51, 5978 (2012).
[5] Puszka, A., Di Sieno, L., Dalla Mora, A., Pifferi, A., Contini, D., Boso, G., Tosi, A., Hervé, L., Planat-Chrétien, A., Koenig, A., and Dinten, J.-M., "Time-resolved diffuse optical tomography using fast-gated single-photon avalanche diodes," Biomed. Opt. Express 4, 1351-1365 (2013).
[6] Boso, G., Dalla Mora, A., Della Frera, A., and Tosi, A., "Fast-gating of single-photon avalanche diodes with 200ps transitions and 30ps timing jitter," Sensors Actuators A Phys. 191, 61–67 (2013).
[7] Tosi, A., Dalla Mora, A., Zappa, F., Gulinatti, A., Contini, D., Pifferi, A., Spinelli, L., Torricelli, A., and Cubeddu, R., "Fast-gated single-photon counting technique widens dynamic range and speeds up acquisition time in time-resolved measurements.," Opt. Express 19, 10735–46 (2011).
[8] Hervé, L., Planat-Chrétien, A., Di Sieno, L., Berger, M., Puszka, A., Dalla Mora, A., Contini, D., Boso, G., and Dinten, J.-M., "Multi-wavelength and time-domain diffuse optical tomography data processing by using a material basis and Mellin-Laplace transform," Proc. SPIE 8952, Biomed. Appl. of Light Scattering VIII, 89520D (2014).